JASMAC Conference of the Japan Society of Microgravity Appllication

OS3-2

化学工学的手法に基づく光触媒反応利用高度空気浄化技術の開発と応用

Development and Application of an Advanced Air Purification Technique Based on Photocatalytic Reaction Through Chemical Engineering Methodology

白石文秀
Fumihide SHIRAISHI[1]
九州大学, Kyushu University

1. Introduction

The air inside buildings is more or less contaminated by various kinds of volatile organic compounds (VOCs)[1,2]. Even when these chemical substances are at low concentration levels, human health is damaged by repeated exposure over a long period of time, and this problem still remains unsolved. Many types of air purifiers are commercially available to decompose and/or remove VOCs. However, their performances (rate of decrease in VOC concentrations and finally reachable minimum concentrations) are not satisfactory. Difficulties in purifying air containing VOCs can be attributed to their low concentrations (normally less than 1 ppm)[3,4]. For instance, when VOC is present in the air at 1 ppm, this corresponds to the state where only one VOC molecule is present in one million air molecules. Therefore, it is very difficult to catch and treat the VOC molecules and then reduce their concentrations toward zero. There is also a severe assignment in which the amount of air to be treated is large.

The Ministry of Health, Labor and Welfare of Japan has set guidelines for 13 VOCs in indoor air in 2003. However, there was no air purifier that can clear the guidelines until recently, and the guidelines are still in an uncontrolled state. I have been studying photocatalytic reactions in both gas and liquid systems since 25 years ago. In this research process, I found that 1) the presence of a static, thin air layer in the very neighborhood of photocatalyst significantly reduces the rate of photocatalytic decomposition[5-9], and 2) it is necessary to always keep the UV intensity per unit surface area of photocatalyst at a high level in order to decompose VOC at a low concentration to a further low concentration [3,10,11]. Moreover, I indicated that these problems can be solved by the use of a photocatalytic reactor with a parallel array of reaction tubes, where the photocatalyst is positioned at or close to the inside surface of a circular tube and is irradiated with UV from a UV lamp in the center of the tube to efficiently decompose VOCs[3,5,11].

I should emphasize that application of chemical engineering methodology greatly contributed to the development of this air purifier. Based on the principle of the treatment, my research group has successfully put the air purifier into market several years ago. If there is no additional discharge of VOCs from architectural materials, the developed air purifier can reduce indoor VOC concentrations to below the guidelines[8,9,12].

Habitat stations constructed in outer space to carry out life-supporting activity are semi-biological systems. In the international space station, the indoor air is contaminated by various volatile chemical substances and some of their concentrations are sufficiently high to menace the human life. Unfortunately, there is no effective way to overcome this problem.

In this presentation, I will talk about the development of our air purifier (photocatalytic reactor), the role of chemical engineering methodology[13,14] in this development, the performance of the developed reactor to decompose VOCs, and the applicability of this reactor to the purification of air in a closed biological system constructed in the outer space.

2. Theoretical

2.1 A mathematical model for photocatalytic reaction combined with film diffusion

The development of our air purifier was carried out in parallel with the analysis of experimental data through the chemical engineering methodology. I will mention below one of the mathematical models used in this process.

Let us consider a photocatalytic reactor with a parallel array of reaction tubes (arranged in parallel in three lines and three rows) where the inside surface is covered with TiO_2[11] (Fig. 1). Each tube has a 6W blacklight blue fluorescent lamp in its center. The rotation of an electric fan positioned above the reaction tubes arrayed in parallel generates a suction of indoor air from the bottom of the reactor. VOC in the air is photocatalytically decomposed while flowing through the annular path between the inside tube wall with photocatalyst and a UV lamp in the center. The photocatalytic reactor is placed in a closed room with an air volume of V. The initial concentration of VOC is at C_0. In the reaction tube, VOC in a bulk diffuses through a film in the neighborhood of TiO_2 to its surface and is then decomposed photocatalytically (Fig. 2).

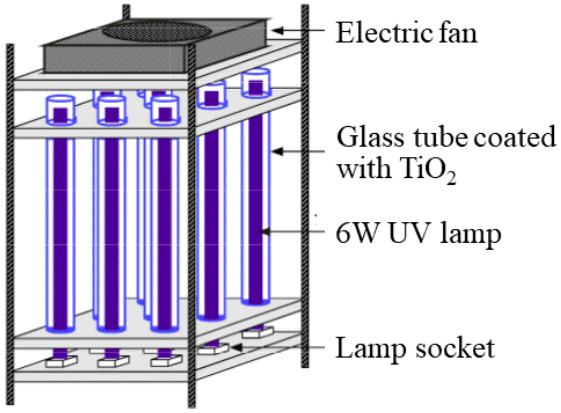

Fig. 1 Photocatalytic reactor with a parallel array of UV lamps.

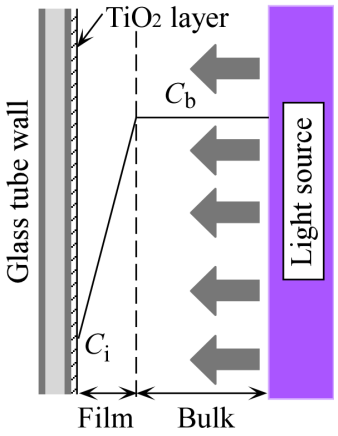

Fig. 2 VOC concentration profile and diffusion film in a circular reaction tube.

The photocatalytic reaction obeys a Langmuir-Hinshelwood kinetics[15]. At a steady state, the present system is described as follows.

$$r = \frac{N k K_H C_i}{1 + K_H C_i} = k_L (C_b - C_i) \tag{1}$$

The time rate of change in the indoor VOC concentration C_b is written as

$$- V \frac{dC_b}{dt} = E_f \frac{N k K_H C_b}{1 + K_H C_b} \tag{2}$$

with the initial condition:

$$C_b = C_{b0} \quad \text{at } t = 0 \tag{3}$$

where k_L is the mass-transfer coefficient, C_i is the VOC concentration at the TiO_2 surface, k is the rate constant per unit reaction tube, N is the number of reaction tubes, K_H is the adsorption equilibrium constant, and t is the time. Also, E_f is the effectiveness factor, given by[16]

$$E_f = \frac{(\beta_b + 1)\{\phi + 1 + \beta_b - \sqrt{(\phi + 1 - \beta_b)^2 + 4\beta_b}\}}{2\phi\beta_b} \quad (4)$$

where $\beta_b = C_b K_H$ and $\phi = K_H N k / k_L$. These are dimensionless parameters. The mass-transfer coefficient, k_L, can be expressed as[17,18]

$$k_L = a u_z^b \quad (5)$$

where u_z is the linear velocity of the air in the reaction tube, and a and b are the experimental constants. To determine the k_L value for each u_z, the difference between the r_0^{exp} values, measured by changing u_z at a constant value of C_0, and the calculated values of r_0^{calc} under the corresponding condition set as

$$f(k_L) = r_0^{calc}(k_L) - r_0^{exp} \equiv 0 \quad (6)$$

where Eq. (6) becomes zero when r_0^{calc} is identical to r_0^{exp}, in other words, the k_L value is correct. The equation for the Newton-Raphson iteration is given as [17]

$$k_L^{(i+1)} = k_L^{(i)} - \frac{f(k_L^{(i)})}{df(k_L^{(i)})/dk_L} \quad (7)$$

where

$$\frac{df(k_L^{(i)})}{dk_L} = \frac{dr_0^{calc}(k_L)}{dk_L} = \frac{1}{V}\frac{N k K_H C_{b0}}{1 + K_H C_{b0}}\frac{dE_f}{dk_L}. \quad (8)$$

The equation for dE_f/dk_L is obtained by differentiating Eq. (4) with respect to k_L.

2.2 Determination of parameters

The parameters in the above equations were determined according to the following procedure.

1) Decompose VOC by changing C_0 under the condition where the air is recirculated at a very high speed to completely remove the film-diffusion resistance, and determine r_0^{exp} from the time course data of the resulting VOC concentration in the initial stage.
2) Determine k and K_H from the linearized plot using C_0 and r_0^{exp}.
3) Implement the Newton-Raphson method using the r_0^{exp} values measured for different values of u_z and calculate the values of k_L and r_0^{calc} that satisfy Eq. (6).
4) Plot the logarithm of k_L against u_z and determine a and b in Eq. (5) by the method of least squares.
5) Apply the determined parameters to Eq. (2) and calculate the r_0^{calc} values for various u_z values
6) Characterize the experimental values by comparing the calculated values with the relationship between r_0^{exp} and u_z.

3. Experimental

3.1 Materials and reagents

Nanosized TiO_2 (Degussa P25) was purchased from Japan Aerosil Co., Ltd. (Tokyo, Japan). Hydrogen peroxide (30 wt% aqueous solution), hexachloroplatinic (IV) acid, palladium(II) nitrate, methanol, formaldehyde, acetaldehyde (AA), toluene, and isopropanol (IPA), plyoxyethylene lauryl ether with a degree of polymerization of 23 were acquired from FUJIFILM Wako Pure Chemical Industry, Ltd. (Osaka, Japan). Standard CO gas (push can type) was procured from GL Sciences Inc. (Tokyo, Japan). AC particles with a mean diameter of 2 mm were used to immobilize TiO_2 (Shirasagi WH2c; Osaka Gas Chemicals Co., Ltd., Osaka). Nine 6-W blacklight blue fluorescent lamps (FL6BLB-A; Toshiba, Tokyo) with a wavelength range of 300–400 nm and nine 6-W germicidal lamps (HC-TK-6; H & C Technical Laboratory Co., Ltd., Kyoto) with a wavelength of 254 nm were used as a light source for the photocatalytic reactions in each glass tube. Stainless steel mesh with an aperture ratio of 67.7 % had wire diameters of 0.25 mm.

3.2 Preparation of the TiO_2-coating solution

Ten grams of fine TiO_2 particles was mixed vigorously with 500 mL of aqueous H_2O_2 solution in a 1 L glass flask. The flask was covered with a sheet of Al foil and was heated at 120 °C for 40 min in a SX-300 (Tomy Seiko Co., Ltd., Tokyo, Japan) high-pressure steam sterilizer to obtain the TiO_2-coating solution[19]. If necessary, hexachloroplatinic(IV) acid (0.2 g), palladium(II) nitrate (0.2 g), and methanol (0.40 M) as photoreducing agent, were added to the flask, and the content of the flask was mixed vigorously for 12 h under UV light irradiation using a 4 W blacklight blue fluorescent lamp under dark. This ensured that Pd and/or Pt deposited on TiO_2, and the obtained product was denoted Pd-Pt/TiO_2 and Pt/TiO_2 [4].

3.3 Kinds of reaction tubes

The obtained coating solution was poured into spiral Pyrex glass tubes (210 mm long and 28 mm i.d.) to cover their inner surfaces. After the excess solution was removed, the tubes were dried in a TMF-2000 (EYELA, Tokyo, Japan) muffle furnace at a temperature of 300 to 500 °C for 30 min. The coating procedure was repeated three times. The resulting reaction tube is referred to as **RT 1**.

The AC particles were dipped into a TiO_2-coating solution, which contained a non-ionic surfactant, polyoxyethylene lauryl ether (0.02 wt%), to increase the affinity between AC and the coating solution. The particles recovered were dried at 100 °C for 30 min. The same coating procedure was repeated twice to yield TiO_2/AC particles; one gram of AC was loaded with 0.14 g of TiO_2. TiO_2 did not detach from AC unless the particles were strongly scrubbed. A stainless steel mesh ($210^L \times 65^W$ mm) was rolled into a cylinder and inserted into the glass tube. The space remaining between the inside wall of glass tube and the stainless steel mesh was packed with 33 g of TiO_2/silica particles or AC particles. A UV lamp was inserted and fixed to the center of the glass tube. The resulting reaction tube is referred to as **RT 2**.

3.4 Photocatalytic reactor and arrangement of reaction tubes

The photocatalytic reactor shown in Fig. 1 was a rectangular box (130 × 130 × 330 mm) with nine reaction tubes arranged in parallel in three lines and three rows. When the electric fan fixed to the top of the box was turned on, air was pulled from the bottom of the reactor at a flow rate of about 2 m^3 min^{-1}.When an electric fan fixed to the top of the box was turned on, air was pulled from the bottom of the reactor at a flow rate of more than 2 m^3 min^{-1}.

3.5 Experiments for VOC decompositions

The photocatalytic reactor was placed in a 1 m^3 closed room covered with transparent vinyl chloride sheets. The room air was vigorously mixed using two electric fans. A predetermined amount of aqueous VOC solution was dropped onto an electrically heated plate and instantaneously evaporated. The room air was sampled after 2 min to determine the initial concentration of VOC. At this point, every light source in the photocatalytic reactor was switched on to initiate the photocatalytic reaction. Air entering the reactor from the bottom was allowed to flow through the annulus of each glass tube at a linear velocity above 11 m s^{-1} [11]. Under this flow condition, the air at the TiO_2 surface is well mixed and VOC is photocatalytically decomposed in the absence of film-diffusion resistance. At given time intervals, a small amount of air was sampled to determine the time course of VOC concentration.

3.6 Analytical method

To accurately measure the HCHO concentration at a level of ppb, air was bubbled into distilled water to trap HCHO. The water containing HCHO was colored using a coloring reagent based on the AHMT method and its absorbance was measured with a spectrophotometer at 550 nm to determine the HCHO concentration. The CO concentration was measured with a CO gas detector (Komyo Rikagaku K. K., Kawasaki, Japan). The CO_2 concentration was measured with a CO_2 detector tube (testo 535; Testo Co., Ltd., Yokohama). The concentrations of other VOCs were measured using a GC-8A (Shimadzu, Kyoto, Japan) gas chromatograph equipped with a flame ionization detector. The sample volume was 3

cm^3 for every VOC. The measurement limits for AA, IPA, toluene, and HCHO were 30, 30, 10, and 20 ppb, respectively.

4 Results and discussion

4.1 Film-diffusion resistance

Fig. 3 presents the relationship between r_0^{exp} and u_z in the treatment of 1 m^3 air containing HCHO at 0.77 ppm using the photocatalytic reactor with nine sets of **RT 1** and BL. The value of r_0^{exp} greatly increased with the increase in u_z and became constant at more than 10 m s^{-1}. This is attributed to a fact that the film in the neighborhood of photocatalyst was disturbed at a significantly-high flow rate of air, by which HCHO became possible to transfer quickly from the bulk to the photocatalyst surface.

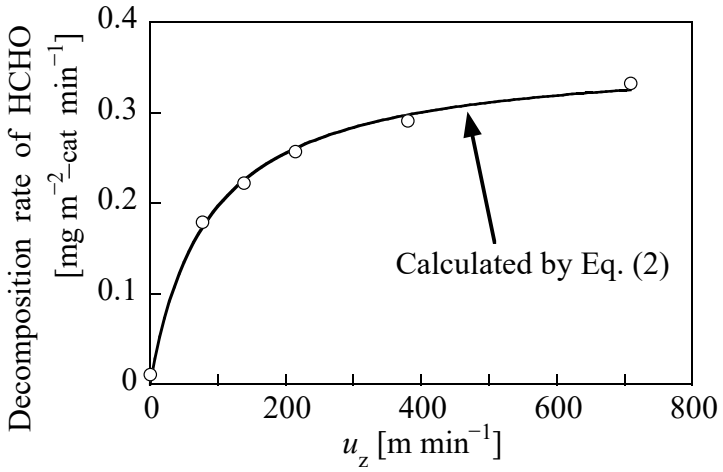

Fig. 3 Relationship between initial rate of decomposition of HCHO and linear velocity in photocatalytic decomposition of HCHO at 0.77 ppm in 1m^3 air.

Chemical engineers mostly consider that chemical substances can quickly diffuse through a gas film and the film-diffusion resistance is generally negligible, so that no attention was entirely paid to the film-diffusion resistance in the photocatalytic reaction system. However, this common sense is incompatible with the experimental result in Fig. 3. Hence, we performed theoretical analysis using the mathematical model described in Section 2.1. The calculated result, represented by a solid line in Fig. 3, is in good agreement with the variation in the experimental data. It is thus evident that the film-diffusion resistance greatly affects the photocatalytic reaction. This can be attributed to the fact that VOCs are present at low concentrations in the environment, by which the difference between the VOC concentrations in the bulk and at the photocatalyst surface is very small, leading to significantly slow diffusion and then increasing the film-diffusion resistance greatly in spite of gas phase reaction.

4.2 UV intensity per unit surface area

UV irradiation excites TiO_2 and generates OH radicals. In order to rapidly decompose VOC in the air and decrease its concentration to zero, it is necessary to increase the density of OH radicals on the photocatalyst surface. BL (300 – 400 nm) or GL (254nm) is widely used as a UV light source for the photocatalytic reaction. For instance, a 20W UV lamp discharges a larger amount of UV than does a 6W UV lamp. However, the UV intensity per unit surface area is higher with the latter lamp than with the former one (Fig. 4). This property greatly contributes to decreasing the VOC concentration to almost zero [3]. Therefore, we selected 6W UV lamps to excite TiO_2.

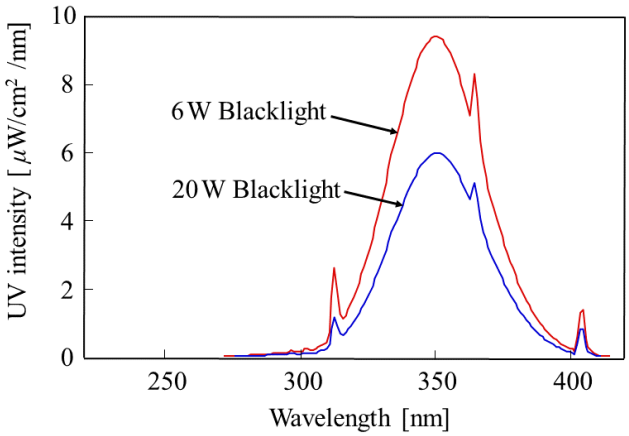

Fig. 4 UV intensity distributions per unit surface for two blacklight blue fluorescent lamps.

4.3 Structure of a photocatalytic reaction field

It is common that the photocatalytic reactor for purifying the air is designed as an apparatus in a multi-shelf structure where several porous plates with the surfaces covered with TiO_2 are arranged in a vertical direction and several UV lamps are put between them. This is based on an imagination that the flat surface easily makes it possible to immobilize a large amount of TiO_2, UV is efficiently utilized in the multi-shelf structure because TiO_2 on neighboring two plates is simultaneously irradiated with UV lamps in between, and the apparatus is easy to manufacture and maintain. As illustrated in Fig.5, the multi-shelf structure produces a distribution of UV intensity on the TiO_2-covered plate, so that the rate of photocatalytic decomposition is lowered, the VOC concentration is never decreased to zero, and VOC and intermediates during the photocatalytic reaction are probably accumulated on a part of the photocatalyst surface with low UV intensity[3]. In contrast, the circular structure, where TiO_2 is positioned on the inside wall of a circular tube or in its neighborhood and a UV lamp is put in the center, provides advantages that VOC is completely decomposed into CO_2 and the VOC concentration is finally decreased to zero. Therefore, we used the circular structure for our photocatalytic reactor.

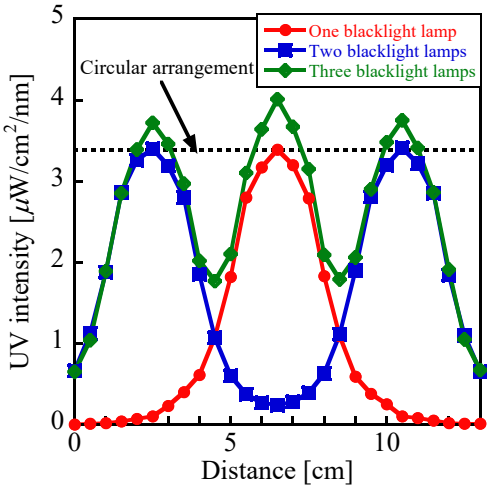

Fig. 5 UV intensity distributions on photocatalysts immobilized on flat plates.

4.4 Performance of the developed air purifier

Fig. 6 presents the experimental result for the photocatalytic decomposition of AA using the photocatalytic reactor with two sets of **RT 1** and GL. The AA concentration decreased to below the detection limit in 60 min; we have confirmed that the time for complete decomposition can be further shortened by increasing the number of reaction tubes. Fig. 7 presents the time courses of HCHO concentration in the treatment of air containing HCHO at different concentrations using the photocatalytic reactor with nine sets of **RT 2** and BL. When no UV lamps were turned on, the HCHO

concentration initially decreased quickly because of adsorption of HCHO on AC particles, but the system reached a steady state soon and the HCHO concentration stopped to decrease (Fig. 7(a)). When the UV lamps were turned on, its detection limit (20 ppb) because of the photocatalytic decomposition (Fig. 7(b)). Similarly, IPA and toluene were decomposed to below their detection limits. These experimental results indicate that the photocatalytic decomposition method is effective for advanced purification of air. IPA and toluene were completely decomposed into CO_2 when their initial concentrations were equal to or less than 1 ppm. HCHO was also decomposed completely when its initial concentration was equal to or less than 5 ppm. These results indicate that when the VOC concentration was low, VOC was rapidly attracted by AC and completely decomposed while diffusing through the TiO_2 layer formed on the AC particles. No intermediates were detected in the decompositions of HCHO and AA, like the case of toluene[3]. Consequently, it is clear that the high performance of the developed photocatalytic reactor is due to the high UV intensity per unit surface area and removal of film-diffusion resistance.

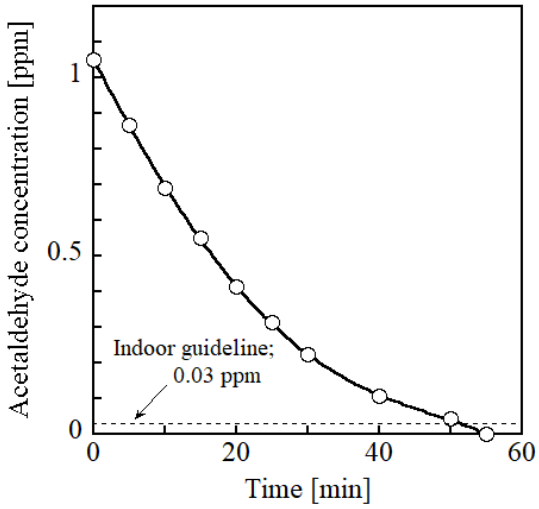

Fig. 6 Photocatalytic decomposition of AA using a photocatalytic reactor with two sets of **RT 1** and GL.

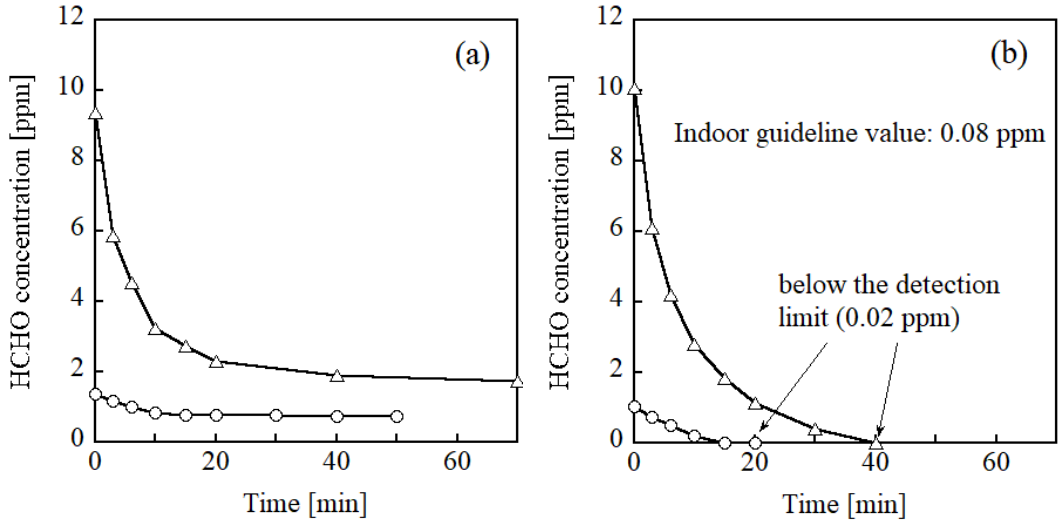

Fig. 7 Treatments of air containing HCHO using a photocatalytic reactor with nine sets of **RT 2** and BL; (a) UV lamps switched off and (b) UV lamps switched on.

4.5 Performance of commercially-available air purifiers

Fig. 8 presents the experimental result for the photocatalytic treatment of air containing AA at 1 ppm using commercially-available air purifiers. The apparatus A in a multi-shelf structure did not entirely decrease the AA

concentration. The apparatus A and B quickly decreased the AA concentration in the initial stage, but immediately stopped decreasing the concentration. The quick decreases in the initial stage are owing to adsorption of AA onto AC filters. The results imply that the VOC-decomposing systems used in these apparatus did not entirely function. The apparatus B in a multi-shelf structure slowly decreased the AA concentration. In contrast, our air purifier (IQ fresher; I-Quark Co., Ltd., Fukuoka, Japan) steadily decreased the AA concentration to below the detection limit. Although two sets of **RT 2** and GL were used in this experiment, it is possible to shorten the time for complete decomposition by increasing the number of reaction tubes.

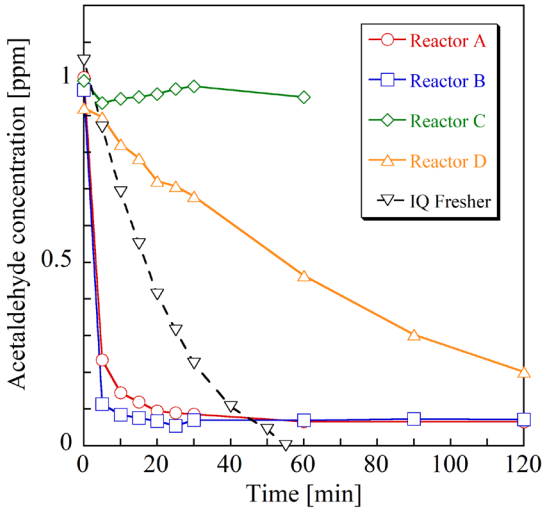

Fig. 8 Treatments of air containing AA at 1 ppm using commercially available air purifiers.

4.6 Applicability of the developed air purifier to purification of air in a closed system in outer space

The air in the space station is highly contaminated with various chemical substances. Hence, it is useful to investigate the applicability of our air purifier. Fig. 9 presents the experimental result for the treatment of air containing CO at 10 ppm using the photocatalytic reactor with nine sets of **RT 2** and GL. The photocatalyst was in the form of Pd-Pt/TiO_2. CO was stoichiometrically oxidized to CO_2. We also confirmed complete decompositions of methyl mercaptan and trimethylamine, and complete removal of NH_3 after photocatalytic oxidation into NO_x followed by removing it using a special type of AC. Methane was not oxidized and therefore other method should be introduced.

In conclusion, it is possible to decompose many kinds of chemical substances using our air purifier. However, since their concentrations are high, it is necessary to further enhance its performance before practical application.

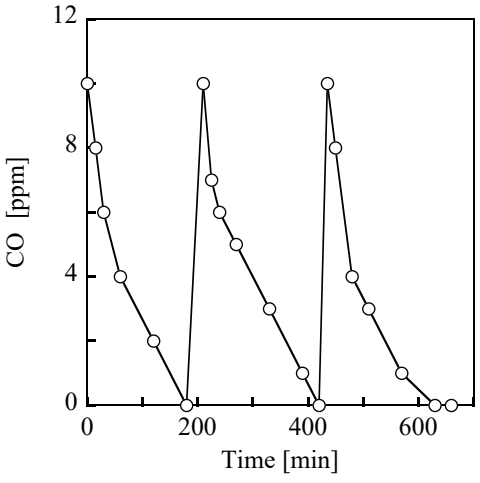

Fig. 9 Repeated treatment of air containing CO at 10 ppm using a photocatalytic reactor with nine sets of **RT 2** and GL.

Acknowledgement

I thank Mr. Kenji Tateishi, Mr. Hirotoshi Kai, and Mr. Tanaka Kenta at I-Quark Co. Ltd. for supporting me to construct and improve photocatalytic reactors.

References

1) K. Ikeda, Mechanism of indoor air contamination, Kajima Institute Publishing, Tokyo, 1992.
2) T. Godish, Sick buildings: definition, diagnosis and mitigation, CRC Press, Florida, 1995.
3) F. Shiraishi, D. Maruoka and Y. Tanoue, Sep. Purif. Technol., **175** (2017) 185.
4) M. Iwanaga, Y. Akimoto and F. Shiraishi, Eco-Eng., **31** (2019) 37.
5) F. Shiraishi, S. Yamaguchi and Y. Ohbuchi, Chem. Eng. Sci., **58** (2003) 929.
6) F. Shiraishi, T. Nomura, S. Yamaguchi and Y. Ohbuchi, Chem. Eng. J., **127** (2007) 157.
7) F. Shiraishi and T. Ishimatsu, Chem. Eng. Sci., **64** (2009) 2466.
8) F. Shiraishi, S. Ikeda and N. Kamikariya, Chem. Eng. J., **148** (2009) 234.
9) F. Shiraishi, N. Kamikariya and Y. Shibata, J. Chem. Technol. Biotechnol., **86** (2011) 852.
10) F. Shiraishi, D. Ohkubo, K. Toyoda and S. Yamaguchi, Chem. Eng. J., **114** (2005) 153.
11) F. Shiraishi, K. Toyoda and H. Miyakawa, Chem. Eng. J., **114** (2005) 145.
12) F. Shiraishi, M. Iwanaga, N. Kitagawa and F. Miyazaki, J. Chem. Tech. Biotechnol., in press (2020)
13) R.B. Bird, W.E. Stewart and E.N. Lightfoot, Transport phenomena, John Wiley & Sons, Inc., 1960.
14) O. Levenspiel, Chemical reaction engineering, John Wiley & Sons, New York, 1962.
15) J.-H. Xu and F. Shiraishi, J. Chem. Technol. Biotechnol., **74** (1999) 1096.
16) F. Shiraishi, Computational methods for analysis of immobilized enzyme reactions, Corona, Tokyo, 1997.
17) F. Shiraishi and M. Hiromitsu, T. Hasegawa and S. Kasai, J. Chem. Tech. Biotechnol., **66** (1996) 405.
18) H. Miyakawa and F. Shiraishi, J. Chem. Tech. Biotechnol., **69** (1997) 456.
19) Y. Tanoue and F. Shiraishi, Eco-Eng., **29** (2017) 39.